

Measurement of the nonlinear Meissner effect in superconducting Nb films using a resonant microwave cavity: A probe of unconventional pairing symmetries

Nickolas Groll,^{1,2} Alexander Gurevich,² and Irinel Chiorescu^{1,2}

¹*Department of Physics, Florida State University, Tallahassee, Florida 32306, USA*

²*The National High Magnetic Field Laboratory, Florida State University,
1800 E. Paul Dirac Drive, Tallahassee, Florida 32310, USA*

(Dated: published 11 January 2010 in *Physical Review B Rapid Comm.* **81**, 020504(R) (2010))

We report observation of the nonlinear Meissner effect (NLME) in Nb films by measuring the resonance frequency of a planar superconducting cavity as a function of the magnitude and the orientation of a parallel magnetic field. Use of low power rf probing in films thinner than the London penetration depth, significantly increases the field for the vortex penetration onset and enables NLME detection under true equilibrium conditions. The data agree very well with calculations based on the Usadel equations. We propose to use NLME angular spectroscopy to probe unconventional pairing symmetries in superconductors.

PACS numbers: 74.25.-q, 74.25.Ha, 74.25.Op, 74.78.Na

Meissner effect is one of the fundamental manifestations of the macroscopic phase coherence of a superconducting state. Meissner screening current density $\mathbf{J} = -en_s \mathbf{v}_s$ induced by a weak magnetic field is proportional to the velocity \mathbf{v}_s of the condensate. At higher fields, the superfluid density n_s becomes dependent on \mathbf{v}_s due to pairbreaking effects, resulting in the nonlinear Meissner effect (NLME) [1–5]. NLME has attracted much attention since it probes unconventional pairing symmetries of moving condensates, for example, the d -wave pairing in cuprates or multiband superconductivity in pnictides. For a single band isotropic type-II superconductor, the NLME at $\mathbf{v}_s \ll \hbar/m\xi_0$ is described by,

$$\mathbf{J} = -\frac{\phi_0 \mathbf{Q}}{2\pi\mu_0\lambda_0^2}(1 - a\xi_0^2 Q^2), \quad (1)$$

where λ_0 is the London penetration depth, ξ_0 is the coherence length, $\mathbf{Q} = \mathbf{v}_s/m\hbar = \nabla\theta + 2\pi\mathbf{A}/\phi_0$, m is the quasiparticle mass, θ is the phase of the order parameter, \mathbf{A} is the vector potential, ϕ_0 is the flux quantum.

NLME can manifest itself in a variety of different behaviors, which reveal the underlying pairing symmetry. For instance, Eq. (1) describes a clean d -wave superconductor at high temperatures $k_B T > p_F v_s$ or a d -wave superconductor with impurities, where p_F is the Fermi momentum [2–4], while in the clean limit at $k_B T < p_F v_s$, the nonlinear term in Eq. (1) takes the singular form $\simeq a_d \xi |Q|$ [2]. In the s -wave clean limit, the NLME is absent at $T \ll T_c$ where $a \propto \exp(-\Delta/T)$ [6], but in the dirty limit $a \sim 1$ even for $T \rightarrow 0$. In multiband superconductors NLME can probe the onset of nonlinearity due to the appearance of interband phase textures suggested for MgB_2 [7] or the line nodes and interband sign change in the order parameter or mixed s - d pairing symmetries, which have been discussed recently for iron pnictides [8].

To date, experiments aiming to observe the NLME in high- T_c cuprates and other extreme type-II superconductors have been inconclusive [9–11] mostly because of

a very small field region of the Meissner state. Since NLME becomes essential in fields H of the order of the thermodynamic critical field $H_c = \phi_0/2\sqrt{2}\pi\mu_0\lambda_0\xi_0$ [1], penetration of vortices above the lower critical field $\mu_0 H_{c1} = (\phi_0/4\pi\lambda_0^2)(\ln\kappa + 0.5) \ll \mu_0 H_c$ imposes the strong restriction $H < H_{c1}$, which reduces the nonlinear correction in Eq. (1) to $\sim (H_{c1}/H_c)^2 \sim \kappa^{-2} \ll 1$, where $\kappa = \lambda_0/\xi_0$ is the Ginzburg-Landau parameter. Yet even small NLME terms in Eq. (1) result in intermodulation effects [3] under strong ac fields, as observed in $\text{YBa}_2\text{Cu}_3\text{O}_{7-x}$ [12]. However, it remains unclear to what extent the intermodulation probes the true equilibrium NLME, not masked by the nonequilibrium kinetics of gapless nodal quasiparticles excited by sufficiently strong ac field [13]. These features may contribute to some insufficiencies in experimental attempts to observe NLME both in magnetization [10, 11] and intermodulation [12] experiments.

In this Rapid Communications we report the observation of NLME, using a method which resolves the problems of vortex penetration and nonequilibrium effects. This opens up the opportunity of probing NLME in any type-II superconductor under true equilibrium conditions. In the method illustrated by Fig. 1 the resonance frequency $f = 1/2\pi\sqrt{LC}$ of a thin film planar cavity is measured as a function of a parallel dc magnetic field H_p . Here C is the strip-to-ground capacitance, $L = L_g + L_k$ is the total inductance, L_g is the geometrical inductance, and $L_k(H_p)$ is the field-dependent kinetic inductance of the superconducting condensate measured by this technique. For a film of width w , length s and thickness $d \ll \lambda_0$, we have $L_k = \mu_0 s G \lambda_0^2 / wd$ (Ref. [14]) where $G \sim 1$ is a geometrical factor [15]. The field-induced increase of $\lambda(H)$ yields the frequency shift $\delta f(H_p) = -\delta L_k f / 2L$ or

$$\delta f/f = -\mu_0 s G [\lambda^2(H_p) - \lambda(0)^2] / 2Ldw. \quad (2)$$

The variation of L_k is detected here using a very low

rf level inside the cavity (estimated to be $\simeq 10$ pW at resonance), which makes it possible to measure the field-induced shift with high precision and sensitivity $\sim 10^{-3} - 10^{-4}$ in the linear response mode. Another key feature of this approach is the use of thin films of thickness $d < \lambda_0$ for which $\mu_0 H_{c1} = (2\phi_0/\pi d^2) \ln(d/\xi_0)$ can be much higher than the bulk $\mu_0 H_{c1}$ [16]. As a result, NLME becomes much more pronounced as stronger fields can be applied without masking NLME by penetration of vortices. The NLME enhancement factor in a thin film can be evaluated from $Q(z) = 2\pi\mu_0\lambda_0^2 J(z)/\phi_0$ induced by the Meissner current density, $J(z) = H \sinh(z/\lambda_0)/\lambda_0 \cosh(d/2\lambda_0)$, which gives the maximum Q at the surface $Q_m^{film} = \pi d\mu_0 H_{c1}^{film}/\phi_0$ for a thin film with $d \ll \lambda_0$, and $Q_m^{bulk} = 2\pi\lambda_0\mu_0 H_{c1}^{bulk}/\phi_0$ for a thick film $d \gg \lambda_0$ at their respective lower critical fields. Hence, the enhancement factor $r = (Q_m^{film}/Q_m^{bulk})^2 = (dH_{c1}^{film}/2\lambda_0 H_{c1}^{bulk})^2 = [4\lambda_0 \ln(d/\xi_0)/d(\ln \kappa + 0.5)]^2$ increases significantly as the film thickness decreases (for a YBCO film with $d = 50$ nm, $\lambda_0 = 200$ nm and $\xi = 2$ nm, we obtain $r \simeq 10^2$). The NLME contribution in Eq. 1 can be regarded as an effective increase of $\lambda^2(H)$ from the zero-field $\lambda^2(0)$ to the maximum $\lambda^2(H_{c1}) = \lambda^2(0)[1 + a(4\xi \ln(d/\xi)/d)^2]$. Thus, NLME in a thin film is no longer cut off by low H_{c1} , which can make the singular Yip-Sauls contribution [2] in d -wave superconductors at $k_B T \ll v_s p_F$ much more pronounced.

Rotating the field in the plane of the film gives rise to an orientational dependence of $\lambda(H)$. This effect is illustrated by Fig. 1(b): the field \mathbf{H}_p inclined by the angle φ relative to the strip axis induces Meissner currents J_x and J_y of which only J_x along the strip couples linearly with the weak rf current $\delta J_\omega \ll J_x$. For a wide film $w \gg \lambda_0^2/d$, we have $Q_x = q(y, t) + pz \sin \varphi$, $Q_y = pz \cos \varphi$, $p = 2\pi\mu_0 H_p/\phi_0$ and $q(y, t)$ is due to the rf current along the film. Linearizing Eq. (1) in q and averaging over the film thickness, we calculate the weak rf current $\delta I_\omega = -\phi_0 d \int_0^w q(y) dy / 2\pi\mu_0 \lambda^2(H)$, which defines the field-dependent $\lambda(H)$,

$$\lambda^2(H_p) = \lambda(0)^2 \left[1 + \frac{a}{3} \left(\frac{2\pi\mu_0 H_p \xi_0 d}{\phi_0} \right)^2 (2 - \cos 2\varphi) \right]. \quad (3)$$

The constant a will be calculated below for the s -wave dirty limit. Here we emphasize two points: (1) rf currents excited in the stripline only probe the NLME caused by the strong dc Meissner screening currents uniform in the plane of the film; (2) the NLME correction is quadratic in d and in H_p , and exhibits a $\cos 2\varphi$ dependence, so that the NLME is minimum for the in-plane field applied along the strip axis.

We demonstrate the angular dependence of NLME in a Nb film with $\kappa \approx 25$. The film has a length $s = 3$ mm, width $w = 100$ μm , thickness $d = 65$ nm, $T_c = 7.25$ K, and the resistivity $\rho_n(T_c) = 23.2$ $\mu\Omega\text{cm}$. The reduced T_c is characteristic of Nb dirty thin films [17]. The length of

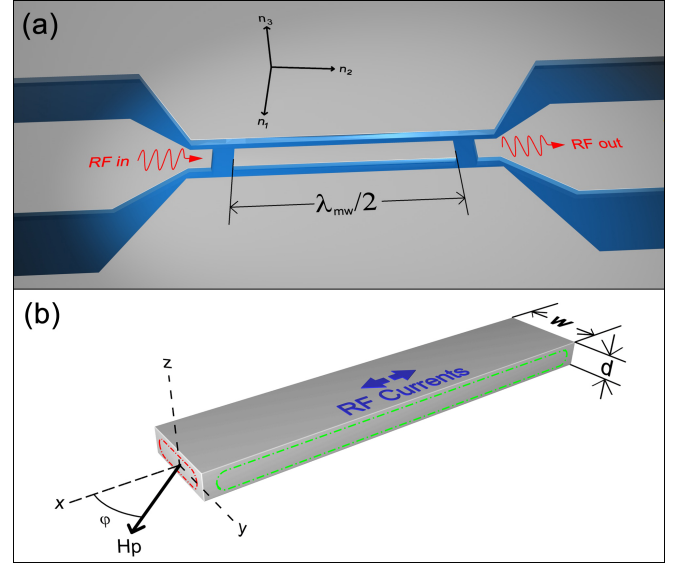


FIG. 1: (a) Cavity sketch as defined by the two RF ports (gaps) separated by half-wavelength $\lambda_{mw}/2 = 3$ mm in an on-chip 50Ω coplanar waveguide. The unit vectors $\hat{n}_{1,2,3}$ show the coil axes. (b) Geometry of a thin film strip in a parallel field H_p , which produces the Meissner screening current loops depicted by dashed lines.

the cavity corresponds to the half-wavelength resonant mode at ~ 20 GHz. The experimental setup is based on a heterodyne detector sensing microwaves transmitted through the two ports of the on-chip superconducting cavity, as illustrated by Fig. 1(a) (similar microwave techniques have been implemented to detect X-rays in astronomy [18] or quantum states of superconducting qubits [19]). Measurements were performed at 80 mK in a Leiden Cryogenics dilution refrigerator.

The challenge with the observation of NLME in a film is to eliminate the significant contribution from perpendicular vortices caused by the field misalignment with the film surface. This was achieved by aligning the film with the magnetic fields of three coils which produce a superposition of the orthogonal fields H_i oriented along the unit vectors $\hat{n}_{1,2,3}$ depicted in Fig. 1(a). To counteract the film misalignment by a proper field rotation, we performed measurements of the frequency shift δf as a function of the nearly perpendicular field H_3 for different in-plane field components (H_1, H_2). The observed linear dependence of $\delta f(H_3)$ shown in Fig. 2 is consistent with the conventional behavior of $\lambda^2(H)$ determined by rf dynamics of pinned perpendicular vortices at low fields for which the critical current density is independent of H_3 [5, 20]. At fixed H_2 and variable H_3 , the slope of $\delta f(H_3)$ abruptly changes sign at the values of H_2^*, H_3^* corresponding to the exact in-plane field orientation. Similar results were obtained in the (H_1, H_3) plane (not shown). This analysis gives the misalignment angles between the field components H_1 and H_2 and the

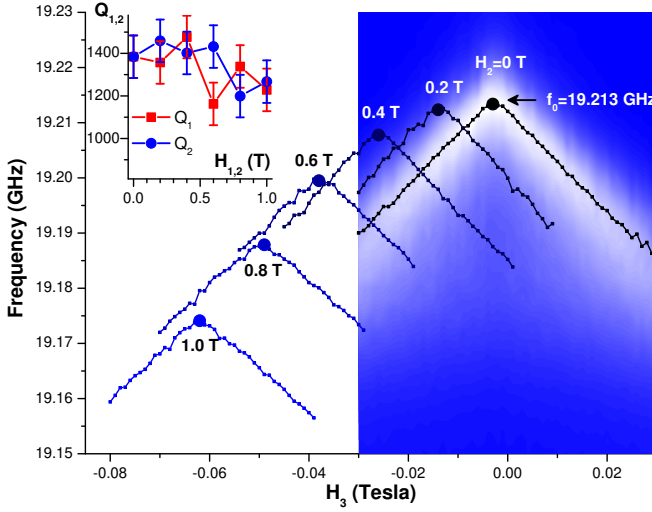


FIG. 2: Contour plot of amplified cavity transmission for variable H_3 field while $H_2 = 0$ T (blue/gray: $0 \mu\text{W}$, white: $6.7 \mu\text{W}$). Scans maxima are shown by small squares, and are repeated for various H_2 (the other contour plots are omitted for clarity). The maxima amongst a group of scans of given H_2 is shown by large dots and indicate an in-plane field position achieved by a specific (H_2^*, H_3^*) combination. Similar measurements are performed for the (H_1, H_3) field combination (not shown). Inset: quality factors $Q_{1,2}$ for (H_1^*, H_3^*) (squares) and (H_2^*, H_3^*) (dots) fields, respectively.

film plane, $\theta_1 = 6.85^\circ \pm 0.02^\circ$ and $\theta_2 = 3.42^\circ \pm 0.02^\circ$, respectively. The observed equal slopes of $\delta f(H_3)$ for all accessible fields $H_{1,2}$ indicate that the effect of the perpendicular field is decoupled from the shift caused by the in-plane field. Moreover, the quality factors for the frequency scans for different in-plane fields $(H_{1,2}^*, H_3^*)$ are essentially field independent, as shown in inset of Fig. 2. This result provides one more evidence that at $(H_{1,2}^*, H_3^*)$ no dissipation caused by possible penetration of vortices occurs up to 1 T, and the film is in the Meissner state.

The main experimental evidence for NLME is shown in Fig. 3 in which the frequency shift is plotted as a function of the in-plane field H_p . The $(H_{1,2}^*, H_3^*)$ maxima amongst scans of fixed $H_{1,2}$ exhibit noticeable shifts towards lower frequencies. For instance, for the data presented in Fig. 2, the decrease from the zero-field $f_0 = 19.213$ GHz to 19.174 GHz at $H_2 = 1$ T gives a relative shift of -0.2% . Similarly, a relative shift of -0.58% is obtained for the scans in the (H_1, H_3) plane at $H_1 = 1$ T (last data point in Fig. 3(a)). The quadratic dependence of δf on H_p shown in Fig. 3(a) is consistent with Eq. (3).

The NLME angular dependence is measured by rotating a constant field H_p within the sample plane, while monitoring continuously the resonance frequency $f(H_p)$. Transmission scans obtained for an 180° rotation of a field $H_p = 1$ T are shown as a contour plot in Fig. 3(b) (the resonance peaks are identified by triangles). The frequency shifts at 1 T corresponding to Fig. 3(a) are shown

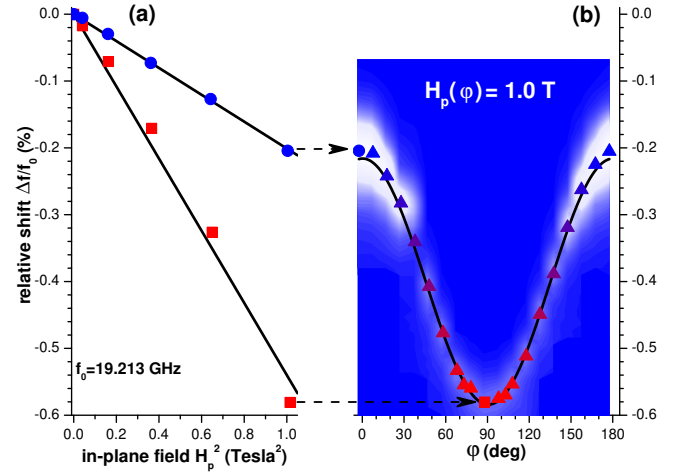


FIG. 3: (a) Relative frequency shift for in-plane field combinations (H_1^*, H_3^*) (squares) and (H_2^*, H_3^*) (dots, taken from Fig. 2) as a function of H_p^2 (lines are through-zero fits). (b) Amplified transmission contour plot as a function of φ (blue/gray: $0 \mu\text{W}$, white: $11 \mu\text{W}$) at constant in-plane field $H_p(\varphi) = 1.0$ T. Maxima, shown by symbols, are in excellent agreement with the theory (black line).

with their original symbols and indicated by the lateral arrows. The 180° periodicity predicted by Eq. (3) is evident. The lines show the fit to the theory described below.

To explain our data quantitatively we calculate $\lambda(H)$ in the dirty s -wave limit by solving the Usadel equations [21] for the energy integrated Green functions, $f_\omega = e^{i\theta} \sin \alpha$, $g_\omega = \cos \alpha$,

$$\frac{D}{2} \left(\nabla^2 \alpha - \frac{Q^2}{2} \sin 2\alpha \right) = \omega \sin \alpha - \Delta \cos \alpha, \quad (4)$$

$$\Delta = 2\pi\gamma T \sum_{\omega>0} \sin \alpha, \quad \mathbf{J} = -2\pi e N D T \mathbf{Q} \sum_{\omega>0} \sin^2 \alpha, \quad (5)$$

where D is the electron diffusivity, γ a pairing constant, ω_D the Debye frequency and N the density of states. For weak current pairbreaking, $\alpha = \alpha_0 + \delta\alpha$ where $\sin \alpha_0 = \Delta / \sqrt{\omega^2 + \Delta^2}$, and $\delta\alpha(z) \propto Q^2$ depends only on z for the planar geometry shown in Fig. 1. Then Eq. (4) gives

$$\delta\alpha'' - k_\omega^2 \delta\alpha = (Q^2/2) \sin 2\alpha_0 - (2\delta\Delta/D) \cos \alpha_0, \quad (6)$$

where $k_\omega^2 = 2\sqrt{\omega^2 + \Delta^2}/D$ and $Q^2(z) = p^2 z^2 + 2pqz \sin \varphi$. In the case of no suppression of Δ at the surface, $\delta\alpha(z)$ in Eq. (6) is a quadratic polynomial of z . Calculating coefficients in this polynomial, the ac current $\delta J(z) \propto q$, and the field-induced gap correction $\delta\Delta \propto Q^2$ from Eqs. (5) and (6), we obtain $\lambda^2(H) = -\phi_0 dq / 2\pi\mu_0 \int_{-d/2}^{d/2} \delta J(z) dz$. For $T = 0$, this yields

$$\lambda^2(H_p) = \lambda_0^2 \left[1 + \left(\frac{2\pi\mu_0 H_p \xi_0}{\phi_0} \right)^2 (C_\varphi d^2 + C_\xi \xi_0^2) \right], \quad (7)$$

$$C_\varphi = (\pi/96 + 1/18\pi)(2 - \cos 2\varphi), \quad (8)$$

where $C_\xi = \pi^2/32 + 7/24 + 1/6\pi$ and $\xi_0^2 = D/\Delta$.

The parameters in Eqs. (2) and (7) can be inferred from independent measurements, except the absolute position of the origin $\varphi = 0^\circ$ relative to the coil axis H_2 . Using the mean-free path extracted from the normal state resistivity, $\ell = \rho^{-1} \times 3.7 \text{ p}\Omega\text{cm}^2 = 1.6 \text{ nm}$ [22], we estimate the dirty limit penetration depth, $\lambda_0 \simeq \lambda(\xi/\ell)^{1/2}(T_{c0}/T_c)^{1/2} = 226 \text{ nm}$, the coherence length $\xi_0 = \sqrt{\xi\ell}(T_{c0}/T_c)^{1/2} = 9 \text{ nm}$, and $\kappa = \lambda_0/\xi_0 \simeq 25$ for the clean-limit values $\lambda \simeq \xi \simeq 40 \text{ nm}$ [23]. Here the factor T_{c0}/T_c accounts for the difference between our sample critical temperature and $T_{c0} = 9.2 \text{ K}$ of pure Nb. We also used the nominal value of the geometrical inductance $L_g = 1295 \text{ pH}$ for which the measured and designed zero field values of f agree very well, and set $G = 1$.

The agreement of our data with Eq. (7) is quite good, as shown in Fig. 3. Here the origin $\varphi = 0^\circ$ was adjusted by 2.5° to account for the misalignment between the strip axis x and the coil axis H_2 . The angular dependence shown in Fig. 3(b) is in excellent agreement with the theory. Also, the two quadratic cavity pulls shown in Fig. 3(a) lead to through-zero fitted slopes of $\delta f/(fH^2) = -5.4 \times 10^{-3} \text{ 1/T}^2$ for $\varphi = 90^\circ$, and $-2 \times 10^{-3} \text{ 1/T}^2$ for $\varphi = 0^\circ$, consistent with the corresponding theoretical values -5.7×10^{-3} and -2.2×10^{-3} . For $d = 65 \text{ nm}$, the in-plane $H_{c1} \approx 0.7 \text{ T}$ is of order of the maximum field used in this study. We have also observed similar NLME behavior for a 40 nm film with $H_{c1} = 1.28 \text{ T}$.

Demonstration of the NLME in conventional high- κ Nb films shows that our method is robust and readily usable to probe unconventional pairing symmetries in other materials. In this case, field rotation in the plane of a thin film strip results in the orientational dependence of $\lambda(H)$ which, in addition to the geometrical factor $2 - \cos 2\varphi$, would contain the intrinsic contribution from the orientational dependence of the order parameter. Separation of the two contributions will reveal the symmetry of the order parameter using the NLME angular spectroscopy proposed in this work. The observation of NLME on a superconductor with $\kappa = 25$ reported here shows that our method is indeed insensitive to low bulk H_{c1} values and can be applied to extreme type-II superconductors. The method can be adapted to study superconducting films made of complex materials, placed on a Nb cavity.

Both types of frequency shifts shown in Figs. 2 and 3 – quadratic NLME due to parallel field and the linear dissipative caused by perpendicular field need to be well understood in research areas requiring precise knowledge of the cavity pull, particularly in quantum computing studies. Quantum spins arranged in small crystals can be entrapped atop of on-chip structures [24] and show relevant multi-photon coherent phenomena [25], but often require strong magnetic fields to control their dynamics. The studies of on-chip superconducting cavities need to take into account the effects reported here.

We have demonstrated the field-dependent non-linear

Meissner effect under true equilibrium conditions in strong dc magnetic fields. The use of thin film resonator cavities opens up opportunities of probing intrinsic symmetries of superconducting order parameter in superconductors using NLME angular spectroscopy.

This work was supported by NSF Cooperative Agreement Grant No. DMR-0654118, NSF grants No. DMR-0645408, No. DMR-0084173, No. PHY05-51164, the State of Florida, DARPA (HR0011-07-1-0031) and the Sloan Foundation. AG is grateful to M.R. Beasley, P.J. Hirschfeld and D.J. Scalapino for discussions and to KITP at UCSB where a part of this work was completed under support of NSF Grant No. PHY05-51164.

-
- [1] V.L. Ginzburg and L.D. Landau, Zh. Exp. Teor. Fiz. **20**, 1064 (1950).
 - [2] S.K. Yip and J.A. Sauls, Phys. Rev. Lett. **69**, 2264 (1992); D. Xu, S.K. Yip, and J.A. Sauls, Phys. Rev. B **51**, 16233 (1995).
 - [3] T. Dahm and D.J. Scalapino, J. Appl. Phys. **81**, 2002 (1997); Phys. Rev. B **60**, 13125 (1999).
 - [4] M.-R. Li, P.J. Hirschfeld, and P. Wölfle, Phys. Rev. Lett. **81**, 5640 (1998); Phys. Rev. B **61**, 648 (2000).
 - [5] R. Prozorov and R.W. Giannetta, Supercond. Sci. Technol. **19**, R41 (2006).
 - [6] J. Bardeen, Rev. Mod. Phys. **34**, 667 (1962).
 - [7] A. Gurevich and V.M. Vinokur, Phys. Rev. Lett. **97**, 137003 (2006).
 - [8] I.I. Mazin and J. Schmalian, Physica C **469**, 614 (2009).
 - [9] C. P. Bidinosti, W. N. Hardy, D. A. Bonn, and R. Liang, Phys. Rev. Lett. **83**, 3277 (1999).
 - [10] A. Bhattacharya, I. Zutic, O. T. Valls, A. M. Goldman, U. Welp, B. Veal, Phys. Rev. Lett. **82**, 3132 (1999).
 - [11] A. Carrington, R.W. Giannetta, J.T. Kim, and J. Giapintzakis, Phys. Rev. B **59**, R14173 (1999).
 - [12] D.E. Oates, S.-H. Park, and G. Koren, Phys. Rev. Lett. **93**, 197001 (2004); D. E. Oates, J. Supercond. Novel Magn. **20**, 3 (2007).
 - [13] N. Kopnin, *Theory of Nonequilibrium Superconductivity*, (Oxford University Press, New York, 2001).
 - [14] T. P. Orlando, K. A. Delin, *Foundations of Applied Superconductivity*, (Prentice Hall, 1991).
 - [15] The factor $G = w \int_0^w J_x^2 dy / (\int_0^w J_x dy)^2 > 1$ accounts for a possible inhomogeneous distribution of rf Meissner currents across a wide film.
 - [16] A. Gurevich, Appl. Phys. Lett. **88**, 012511 (2006).
 - [17] T.R. Lemberger, I. Hetel, J.W. Knepper, F.Y. Yang, Phys. Rev. B **76**, 094515 (2007).
 - [18] P. K. Day, H. G. LeDuc, B. A. Mazin, A. Vayonakis, J. Zmuidzinas, Nature **425**, 817 (2003).
 - [19] A. Wallraff, D. I. Schuster, A. Blais, L. Frunzio, R.-S. Huang, J. Majer, S. Kumar, S. M. Girvin, R. J. Schoelkopf, Nature **431**, 162 (2004).
 - [20] M.W. Coffey and J.R. Clem, Phys. Rev. B **45**, 9872 (1992); E.H. Brandt, Rep. Prog. Phys. **58**, 1456 (1995).
 - [21] K.D. Usadel, Phys. Rev. Lett. **25**, 507 (1970).
 - [22] E.L. Garwin, M. Rabinowitz, Appl. Phys. Lett. **20**, 154 (1972).
 - [23] B.W. Maxfield and W.L. McLean, Phys. Rev. **139**,

- A1515 (1965).
- [24] N. Groll, S. Bertaina, M. Pati, N.S. Dalal, I. Chiorescu, J. Appl. Phys. **106** (4), 046106 (2009).
- [25] S. Bertaina, L. Chen, N. Groll, J. Van Tol, N.S. Dalal, I. Chiorescu, Phys. Rev. Lett. **102**, 050501 (2009).